1   **Carbon isotope fractionation of substituted benzene analogs during oxidation with ozone**

2   **and hydroxyl radicals: How should experimental data be interpreted?**

3   Sarah Willach[†], Holger V. Lutze[†,‡,§], Holger Somnitz[‖], Jens Terhalle[†], Nenad Stojanovic[†], Michelle

4   Lüling[†], Maik A. Jochmann[†,§], Thomas B. Hofstetter[τ,ϒ], Torsten C. Schmidt*[,†,‡,§]

5   [†] University of Duisburg-Essen, Faculty of Chemistry, Instrumental Analytical Chemistry,

6   Universitätsstr. 5, D-45141 Essen, Germany

7   [‡] IWW Water Centre, Moritzstr. 26, D-45476 Mülheim an der Ruhr, Germany

8   [§] University of Duisburg-Essen, Centre for Water and Environmental Research (ZWU)

9   Universitätsstr. 5, D-45141 Essen, Germany

10   [‖] University of Duisburg-Essen, Faculty of Chemistry, Theoretical Chemistry, Universitätsstr. 5,

11   D-45141 Essen, Germany

12   [τ] Eawag, Swiss Federal Institute of Aquatic Science and Technology, Überlandstr. 133, CH-8600

13   Dübendorf, Switzerland

14   [ϒ] Institute of Biogeochemistry and Pollutant Dynamics, ETH Zürich, Universitätstr. 16, CH-8092

15   Zürich, Switzerland

16   *Corresponding author: Tel.: +49 201 183 6774; Fax: +49 201 183 6773; E-mail address:
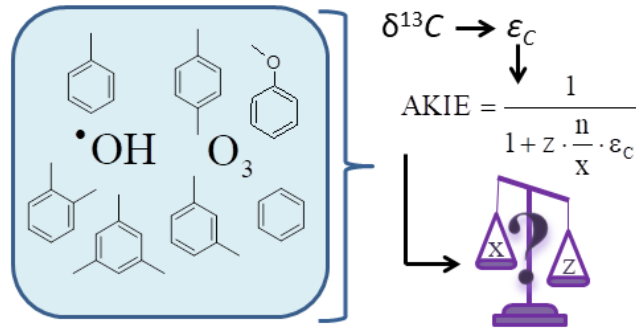
17   torsten.schmidt@uni-due.de

18

Abstract

Oxidative processes frequently contribute to organic pollutant degradation in natural and engineered systems such as during the remediation of contaminated sites and in water treatment processes. Because a systematic characterization of abiotic reactions of organic pollutants with oxidants such as ozonation or hydroxyl radicals by compound-specific stable isotope analysis (CSIA) is lacking, stable isotope-based approaches have rarely been applied for the elucidation of mechanisms of such transformations. Here, we investigated the carbon isotope fractionation associated with the oxidation of benzene and several methylated and methoxylated analogs, namely toluene, three xylene isomers, mesitylene and anisole, and determined their carbon isotope enrichments factors (ε_C) for reactions with ozone (ε_C = −3.6 ‰ to −4.6 ‰) and hydroxyl radicals (ε_C = 0.0 to −1.2 ‰). The differences in isotope fractionation can be used to elucidate the contribution of the reactions with ozone or hydroxyl radicals to overall transformation. Derivation of apparent kinetic isotope effects (AKIEs) for the reaction with ozone, however, was nontrivial due to challenges in assigning reactive positions in the probe compounds for the monodentate attack leading to an ozone adduct. We present several options for this step and compare the outcome to quantum chemical characterizations of ozone adducts. Our data show that a general assignment of reactive positions for reactions of ozone with aromatic carbon in *ortho*-, *meta*- or *para*-positions is not feasible and that AKIEs of this reaction should be derived on a compound-by-compound basis.

39   **Table of contents (TOC)/Abstract Art**

40

$$\delta^{13}C \rightarrow \varepsilon_C$$

$$AKIE = \frac{1}{1 + z \cdot \frac{n}{x} \cdot \varepsilon_C}$$

41

42

Introduction

Oxidative processes play an important role in pollutant degradation in natural[1, 2] and numerous engineered systems such as during the remediation of contaminated sites[3-5] and water treatment processes[6]. In water treatment processes, a broad variety of oxidants are used including chlorine dioxide (ClO_2)[7, 8], ozone (O_3),[6, 9] and hydroxyl radicals ($^\bullet OH$)[6]. Reactions of these oxidants with organic compounds exhibit common features such as the selectivity for electron-rich organic moieties[10] (O_3[6] and ClO_2[7]) and the involvement of radical species ($^\bullet OH$[6] and ClO_2[7]). Common processes to generate significant amounts of $^\bullet OH$ in water treatment, are, e.g., H_2O_2/UV or the peroxone process (O_3/H_2O_2).[6, 11] Usually, oxidative processes cause chemical modifications, e.g. through electron transfer and oxygenation[6, 8] of the persistent pollutants and enable their further degradation[1]. Detecting the resulting oxidation products to assess the utility of oxidative processes in removing pollutants is often challenging and may be hampered if their susceptibility for further oxidation is higher than that of the original contamination. One option to monitor such reactions is compound-specific stable isotope analysis (CSIA).[12, 13]

CSIA is a widely used tool to track the origin and fate of environmental contaminants and to distinguish environmental degradation processes over much longer timescales of years to decades.[12-14] Examples include the monitoring and distinction of biotic and abiotic remediation activities if differences in isotope fractionation of the (bio)transformation processes occur.[3, 12, 13, 15-17] Those distinctions are possible because the isotope effects determining the observable isotope fractionation in a pollutant are indicative of a reaction mechanism.[12] This feature enables one, for example, to differentiate aerobic and anaerobic biodegradation or acid hydrolysis of methyl *tert*-butyl ether (MTBE) from each other - three transformation pathways which otherwise could not be differentiated from the reaction product because those reactions all lead to *tert*-butyl alcohol (*tert*-BuOH).[12, 18] However, up to now only a few studies applied CSIA for investigation of oxidation processes relevant in water treatment.[19-21]

4

68   Isotopic enrichment factors (ε_E) and apparent kinetic isotope effects (AKIE$_E$s) of an isotopic

69   element E are key parameters in CSIA for assessing how contaminants react. Whereas ε_E values

70   enable one to apply and interpret CSIA to specific pollutants, AKIE$_E$s allow for general

71   mechanistic insights into reaction mechanisms.[14, 15, 22, 23] These two parameters are related as

72   specified in eq. 1.[24]

$$\text{AKIE}_E = \frac{1}{1 + z \cdot \dfrac{n}{x} \cdot \varepsilon_E} \tag{1}$$

73   where n is the number of atoms of the considered element (i.e., in this study carbon

74   atoms) of which the number of x atoms are located at a reactive position and z is the number of

75   equivalent reactive positions in intramolecular competition.[24]

76   As a consequence, it is possible to assign certain ranges of AKIEs to specific reaction

77   mechanisms under the assumption that they share one major rate-determining reaction step.[15, 24]

78   Such AKIE ranges would be helpful in environmental or technical process oriented investigations

79   to infer reaction mechanisms of pollutant degradation from ε_E value(s).[15, 24] However, because

80   experimental data is scarce (e.g. [21]) no appropriate ranges for AKIEs originating from oxidation

81   reactions with O_3 or ClO_2 of benzene and its analogs have been defined to date.

82   In order to define the required variables x and z (eq. 1) it is necessary to convey a well-defined

83   hypothesis for the reaction mechanism.[24] Exemplarily, $^\bullet$OH have been found to react with

84   benzene and its analogs either via electrophilic attack at the aromatic moiety or via H abstraction

85   from the substituent.[21, 25] The initial reaction step of the electrophile O_3 was postulated to be a

86   monodentate attack of the aromatic ring leading to adduct formation.[6, 26] After this unique initial

87   reaction step several different pathways are possible as depicted in Scheme S1. Regarding

88   ozonation of benzene and its analogs, it is a general obstacle that their primary ozonation

89   products are muconic (i.e. C_6-ring cleavage products) or phenolic compounds.[6] These products

90 show significantly higher reaction rate constants with O_3 [6] than the respective reactants

91 (< 10^3 M^{-1} s^{-1};[27] Table S1). O_3 reacts with muconic products with a bimolecular rate constant of

92 approximately 10^4 M^{-1} s^{-1}.[6] In case of phenolic compounds (Table S1) (pK_a(phenol) = 9.9)[27], the

93 very fast reaction rate constant of the anion is the reason why traces of phenolate even at

94 neutral pH are sufficient to cause observable reaction rate constants > 10^6 M^{-1} s^{-1}.[6] The reactivity

95 pK_a is found at pH ≈ 4,[6] that is the pH where the reacting quantities of neutral and anionic

96 species are equal. Consequently, it is hardly possible to quantify the primary ozonation reaction

97 products of benzene and its analogs with a reasonable effort which would give insights on the

98 initial point of attack. Hence, a complementary approach such as computational chemistry is

99 required to derive appropriate values for the variables x and z (eq.1).

100 The aim of this study was to elucidate isotopic fractionation trends pertinent to the oxidation

101 reaction of the well-established oxidative processes applied in water treatment (i.e., ozonation,

102 ·OH treatment, and chlorine dioxide) using benzene and its methylated or methoxylated analogs

103 as model compounds for reactive aromatic moieties in organic pollutants. The second objective

104 was to present ^{13}C-AKIE-values, which define characteristic ranges for the oxidation reactions of

105 O_3 with the used model compounds. The determination of AKIEs turned out to be nontrivial and

106 the assignment of reactive moieties for reactions of the probe compound with O_3 is elucidated

107 here with evidence from quantum chemical calculations.

Material and Methods

Chemicals

110 Chemicals and solvents were used as received from the supplier. A complete list of all chemicals

111 used is given in the supporting information (SI) in Text S1.

Generation of ozone stock solutions

O_3 was generated by an O_3 generator BMT 802X (BMT Messtechnik, Berlin, Germany) using oxygen as feed-gas. The O_3 gas was led into an ice cooled impinger filled with ultrapure water. The O_3 stock solution was continuously purged with O_3 gas throughout its utilization. The O_3 concentration of this stock solution was determined spectrophotometrically of a 1:3-diluted O_3 stock solution at 258 nm, ε_{O3} = 3200 M^{-1} cm^{-1}.[6] The resulting O_3 concentrations were in a range of 1.6-1.7 mM O_3.

Sample preparation

The stock solutions of each probe compound including benzene and its analogs for preparation of calibration standards were prepared in methanol. Stock solutions for oxidation experiments with O_3 or ${}^\bullet OH$ were prepared in ultrapure water because the presence of methanol may lead to formation of undesired reactive species such as superoxide radicals ($O_2^{\bullet -}$) which could accelerate O_3 decay due to ${}^\bullet OH$ formation.[28] The aqueous stock solutions were prepared in Erlenmeyer flasks by addition of an aliquot of one pure probe compound to ultrapure water and subsequent shaking for at least 48 h. Due to the limited solubility in water the remaining organic phase was removed thereafter. Final concentrations of the aqueous stock solutions were determined with HPLC-DAD. The aqueous stock solutions were used within a day of their preparation. Reactors were prepared as batch samples in 20-mL headspace screw cap vials. In case of oxidation with O_3 the pH was kept constant at pH 7 with 5 mM phosphate buffer. Additionally, *tert*-BuOH (i.e., 2-methylpropan-2-ol) was added in order to scavenge ${}^\bullet OH$ which may be formed in the reaction with O_3.[6] The *tert*-BuOH concentrations were chosen individually for each compound so that $\geq$ 95 % of ${}^\bullet OH$ formed were scavenged (Text S2 and Table S1). A detailed overview on sample composition is shown in Tables S2-S8. In case of oxidation with ${}^\bullet OH$ the peroxone process was utilized (i.e., ${}^\bullet OH$ are generated by the reaction of O_3 with hydrogen peroxide).[6, 29] The amounts of hydrogen peroxide required to obtain $\geq$ 99 % reaction

137   with O_3 were calculated using the corresponding reaction rate constants (Text S4 and Table S1).

138   Due to the faster reaction rate constant of O_3 with the hydrogen peroxide anion

139    $(k_{O_3+HO_2^-} = 9.6 \times 10^6 \text{ M}^{-1}\text{s}^{-1})$[29] than with the neutral species $(k_{O_3+H_2O_2} < 10^2 \text{ M}^{-1}\text{s}^{-1})$[30], peroxone

140   reaction experiments were carried out at pH 9 $(k_{obs(O_3+HO_2^-)} = 1.5 \times 10^4 \text{ M}^{-1}\text{s}^{-1}$, Table S1). The

141   pH was controlled with a 5 mM borate buffer. The individual sample compositions depended on

142   the reaction rate constants of each benzene analog with O_3 and $^\bullet$OH and are given in SI in

143   Tables S9-S15.

144   A detailed description of oxidation experiments with ClO_2, the respective sample preparation and

145   the generation of the required ClO_2 stock solutions can be found in the SI in

146   Text S6, Tables S16-S22 and Text S5, respectively.

Analytical methods

148   For determination of UV-vis absorption a UV-1650PC spectrophotometer (Shimadzu, Duisburg,

149   Germany) was used with a quartz cuvette with an optical path length of 1 cm. For pH

150   measurements, a pH-meter (827 pH lab with aquatrode both from Metrohm, Herisau,

151   Switzerland) was used which was calibrated with standard buffers every working day.

152   Quantification of benzene and its analogs in the aqueous stock solutions was performed with an

153   HPLC-UV/vis system (LC-20AT coupled to SPD-20A; Shimadzu, Duisburg, Germany). A

154   detailed description can be found in Text S7.

155   Compound-specific stable carbon isotope values of benzene and its analogs were determined

156   by gas chromatography isotope-ratio mass spectrometry (GC-IRMS) which is described in detail

157   in Text S8. Briefly, a Trace GC Ultra coupled by the combustion interface Finnigan GC-C/TC III

158   to a Finnigan MAT 253 isotope ratio mass spectrometer (all from Thermo Scientific, Bremen,

159   Germany) was used. The GC system was additionally equipped with a HTX PAL autosampler

160   (CTC Analytics, Zwingen, Switzerland; supplied by Axel Semrau, Sprockhövel, Germany) with

161 an agitator and an Optic 3 injector (ATAS GL-Sciences, Eindhoven, Netherlands; supplied by

162 Axel Semrau). After sample conditioning in the agitator 500 µL of the headspace were injected.

163 Compounds were separated on a Rxi®-5Sil MS column (60m x 0.25 mm i.d., 0.25 µm film

164 thickness; Restek, Bad Homburg, Germany) using different temperature gradients described in

165 Table S23. After separation, the analytes were oxidized to CO_2 at 940 °C in the combustion

166 interface equipped with Pt, CuO and NiO wires, which were reoxidized each time (i.e., after 40 to

167 60 injections) before a new sample set was run. At least every fourth sample run was a

168 reference sample without oxidant addition for quality control. Linearity and precision tests were

169 run regularly. The carbon isotope values are given in reference to the international Vienna Pee

170 Dee Belemnite (VPDB) scale according to eq. 2 (Text S8).[14]

$$\delta^{13}C_{sample,VPDB} = \left(\frac{R_{sample}(^{13}C/^{12}C) - R_{VPDB}(^{13}C/^{12}C)}{R_{VPDB}(^{13}C/^{12}C)} \right) \qquad (2)$$

171 Where R_{sample} and R_{VPDB} are the ratios of $^{13}C/^{12}C$ of the samples and VPDB, respectively. At

172 least two to three calibrated CO_2 reference gas pulses were included in each chromatographic

173 run for referencing. The peak areas used for the ratio of concentration to initial concentration

174 (c/c_0) originate from the $^{12}CO_2$ peak (*m/z* 44).

175 The carbon isotope enrichment factors (ε_C) of the different oxidation experiments of benzene

176 and its analogs with O_3 or $^\bullet OH$ were determined by application of the Rayleigh equation

177 (eq. 3):[14]

$$\ln\left(\frac{R_{i,sample}(^{13}C/^{12}C)}{R_{0,sample}(^{13}C/^{12}C)} \right) = \ln\left(\frac{\delta^{13}C_{i,sample}+1}{\delta^{13}C_{0,sample}+1} \right) = \varepsilon_C \cdot \ln\left(\frac{c_{i,sample}}{c_{0,sample}} \right) \qquad (3)$$

178 Where $\delta^{13}C_0$ and $\delta^{13}C_i$ and the concentrations of each model compound, i.e. c_0 and c_i, relate to

179 the sampling point *0* (no oxidant added) and sampling point *i* (transformation after full oxidant

180 turnover at defined oxidant doses), respectively.

Quantum chemical calculations

Quantum chemical calculations have been performed to gain more insight into the reactions on a molecular scale.[31] Three scenarios (i.e., calculations type 1-3) have been conducted for further elucidation. All calculations were performed with the Gaussian09 and Gaussian16 program packages[32].

Calculations type 1 focused on the determination of optimized geometries of possible adduct compounds originating from a monodentate attack of ozone on the various substituted benzene derivatives. These calculations were performed at the unrestricted UMP2 level using a moderately sized segmented valence double zeta 6-31+G(2d,p) basis set with polarization functions on all atoms and a set of diffuse functions on non-hydrogens.[33-35] To account for liquid phase conditions all calculations were embedded in a self-consistent reaction field (SCRF) in form of the polarizable continuum model (PCM)[36] assuming water as solvent. In calculations type 1, it turned out that a full set of adduct compounds including a number of different conformers and isomers could only be derived if the electronic triplet state was assumed. In addition, transition states could be located and optimized for the corresponding reverse reactions of ozone cleavage. However, these transition states and adduct molecules correspond to a reactive electronic triplet surface, e.g. accessible by the singlet state benzene derivative plus an exited state triplet ozone molecule.

Calculations type 2 were started to reoptimize the various ozone adduct structures in an open shell singlet electronic state. Again, these calculations made use of the unrestricted UMP2/6-31+G(2d,p) method embedded in a PCM reaction field.[33-36] The unrestricted treatment for the singlet electronic state was forced by mixing alpha and beta molecular orbitals, thus destroying spatial symmetries in the initial guesses of the wave function in every step of the geometry optimization. Unfortunately, only few calculations converged and resulted in the desired singlet state adduct, despite the previously optimized (triplet) starting geometries. In summary, we were

206 able to derive complete triplet state as well as singlet state reaction paths (including transition
207 states) only for triplet/singlet ozone added to benzene and *p*-xylene, respectively. These results
208 were later used to calculate the kinetic isotope effect via statistical reaction kinetics using
209 ISOEFF[37].

210 In calculations type 3, the electronic properties of the various substituted benzene derivatives
211 such as electrostatic potential mapped onto the electron density and regional Fukui functions
212 (Text S9) were derived. Fukui functions were derived with a calculation program,[38] publicly
213 available under GPL 3.0 License in accordance to the work of Contreras et al.[39]. In addition to
214 the already calculated geometries at the PCM/MP2-level (see above) also PCM/B3LYP/6-
215 31++G(2df,p)[40] ones were utilized as base geometries. The corresponding structural
216 optimizations with the B3LYP Hybrid-DFT method[41] along with a slightly larger basis set served
217 as additional check for our previous calculations at the MP2 level.

Results and discussion

Isotope fractionation in transformation of benzene and its analogs

220 Carbon stable isotope values were determined for benzene, its methylated analogs and anisole
221 (methoxybenzene) oxidized with $^\bullet$OH and O_3. The corresponding Rayleigh-plots (eq. 3) are
222 shown in Figure S1. The observed isotopic fractionations always occurred as *normal* isotope
223 effect, that is molecules containing the heavier ^{13}C isotope reacted slower than molecules
224 containing exclusively ^{12}C so that the residual substrate fraction is depleted in molecules with the
225 lighter ^{12}C. As a consequence, the ratio of $^{13}C/^{12}C$ increased as the oxidation reactions
226 proceeded further. The determined ε_C values (eq. 3) for the investigated transformation reactions
227 (i.e., ε_C(oxidation with $^\bullet$OH) ranging between -0.0 ± 0.2 ‰ and -1.2 ± 0.1 ‰ and ε_C(oxidation
228 with O_3) ranging between -3.7 ± 0.1 ‰ and -5.4 ± 0.3 ‰) are shown in Figure 1 and are listed as
229 numerical values in Table S24.

230   Additionally, transformation reactions of benzene and its analogs were conducted with chlorine

231   dioxide (ClO_2) as oxidant (see Text S10 and Figures S2-S8). However, for most of the probe

232   compounds it was not possible to perform experiments that led to a significant reactant

233   transformation. Trends of carbon isotope signatures are lacking and data are shown

234   (Figures S2-S8) and discussed in the SI (Text S10).

235   ## Oxidation with hydroxyl radicals

236   Benzene and its analogs were oxidized with the peroxone process (i.e., with •OH). All resulting

237   ε_C values for benzene and its methylated analogs (Figure 1) were found to be in a similar range

238   of 0.0 to −0.9 ‰. Only, the ε_C value for anisole was somewhat more negative (−1.2 ± 0.1 ‰).

239   This small but still measurable isotope fractionation for oxidation of benzene and its analogs was

240   also observed by Zhang et al. with H_2O_2/UV - another •OH generating water treatment process.[21]

241   The related values are included in Figure 1 and Table S24 to facilitate direct comparison. The

242   slight variations between the ε_C values for each single compound may be attributed to the

243   different experimental setups applied for generation of •OH (i.e., O_3/H_2O_2 (this study) and

244   H_2O_2/UV (Zhang et al.)[21]). For degradation of toluene with the Fenton-like reaction, another •OH

245   based oxidation process, an ε_C value of −0.2 ‰ was determined.[42] Hence, based on these

246   results it is possible to assign a specific range for ε_C values to be expected for •OH based

247   oxidation of benzene and its methylated analogs between 0.0 ‰ and −0.9 ‰.

248
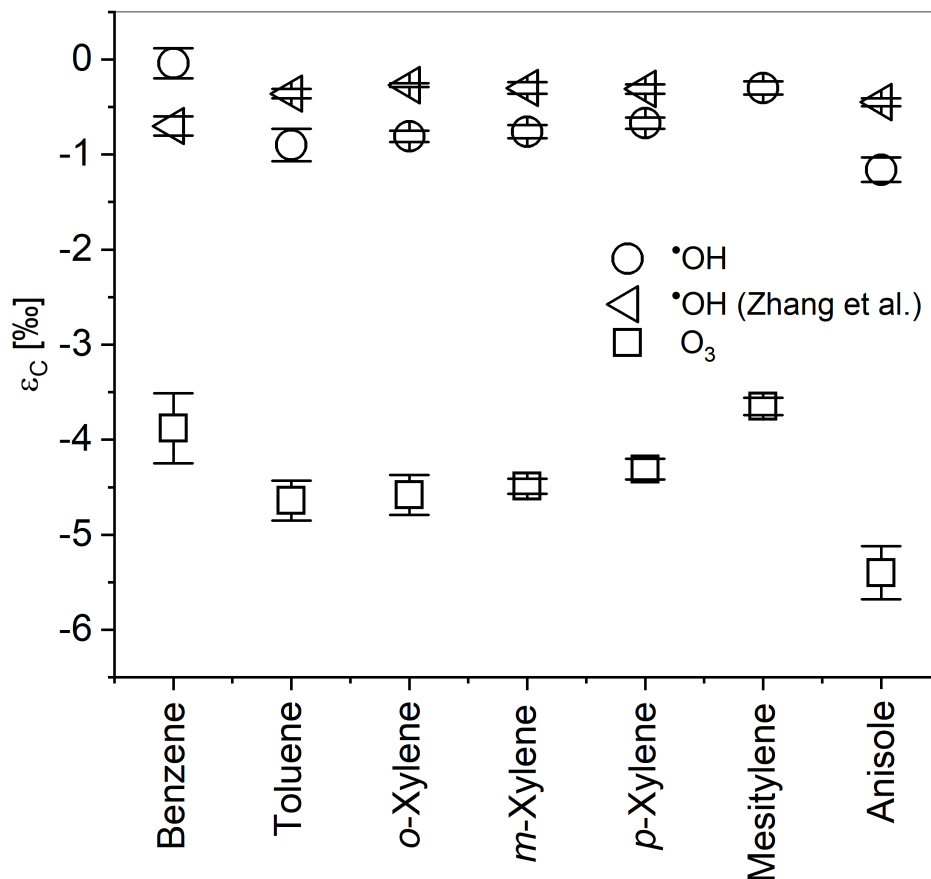
Figure 1: Stable isotope enrichment factors (ε_C) for oxidation of benzene and its analogs with either O_3 or ${}^{\bullet}OH$ (generated by the peroxone process). pH was kept constant, i.e. at pH 9 with 5 mM borate buffer (${}^{\bullet}OH$ reactions, peroxone) and at pH 7 with 5 mM phosphate buffer (O_3 reactions). In oxidations with O_3, intrinsically formed ${}^{\bullet}OH$ after reaction of O_3 with one of the compounds were scavenged with *tert*-BuOH (cf. sample preparation); error bars represent the standard deviation of the slope of each Rayleigh equation. For comparison, ε_C values of oxidation by ${}^{\bullet}OH$ generated by UV/H_2O_2 (triangle leftward; Zhang et al.[21]) are included. Note: Mesitylene was not investigated by Zhang et al.[21].

257

Oxidation with ozone

The ε_C values for oxidation of benzene and its methylated analogs with O_3 are within a range of

1 ‰ (i.e., between −3.6 ‰ and −4.6 ‰) whereas the ε_C for the methoxy analog anisole is even

more negative (i.e. −5.4 ± 0.3 ‰; Figure 1 and Table S24). For the compounds under study, the

ε_C values for the oxidation with O_3 (${}^{\bullet}OH$ excluded) are different from those obtained for oxidation

with ${}^{\bullet}OH$ (< −1 ‰). Hence, a second distinct range for ε_C values (i.e., from −3.6‰ to −4.6‰) may

264   be ascribed for oxidation of benzene and its methylated analogs with O_3. Consequently,

265   oxidation of benzene and its analogs with $^\bullet$OH or O_3 may be differentiated from each other by

266   comparison of ε_C values determined by CSIA. This result is in agreement with the rate constants

267   (Table S1) which already indicated that $^\bullet$OH reactions occur at close to diffusion controlled

268   rates[6], thus resulting in less pronounced ε_C values, whereas O_3 is a more selective oxidant[6]

269   showing elevated ε_C values.

270   These insights from CSIA could be incorporated in future applications of oxidative drinking water

271   treatment to identify the primary oxidation conditions such as for estimating the R_{ct} which is an

272   important parameter to describe ozonation of water and wastewater.[6, 43, 44] The parameter R_{ct}

273   equals the ratio of $^\bullet$OH- and O_3-concentration and exposure, respectively, in an ozonation

274   process (eq 4)[43] (note that $^\bullet$OH are formed in reactions of O_3 with water matrix constituents such

275   as natural organic matter (NOM))[6]. The R_{ct} value mainly depends on the water matrix

276   constituents and the oxidant dose and has to be determined for every individual ozonation

277   process, which requires regular sampling and performing according laboratory experiments.[43]

278   Once the R_{ct} value is known, one can calculate $^\bullet$OH exposures from O_3 exposures (eq. 4). Since

279   O_3 exposures are easily determined online,[44] the R_{ct} value allows to assess also $^\bullet$OH exposures

280   online. With these two exposures at hand, one can monitor disinfection and pollutant

281   degradation during ozonation if according reaction rate constants are available in literature.

$$R_{ct} = \frac{\left[^\bullet OH\right]}{\left[O_3\right]} \tag{4}$$

282

283   where [$^\bullet$OH] and [O_3] are the concentrations or exposures of $^\bullet$OH and O_3, respectively.

284   A complementary approach to determination of the R_{ct} value could be the determination of the ε_C

285   value of e.g. a methylated benzene analog such as mesitylene. The obtained ε_C value would

286 allow conclusions on the oxidative process conditions, that is $\varepsilon_C \geq -0.4\ ‰$ is purely ${}^\bullet$OH

287 governed, $-0.4\ ‰ > \varepsilon_C > -3.6\ ‰$ mixed conditions with a contingent tendency and $\varepsilon_C \leq -3.6\ ‰$

288 purely O_3 governed. By regular verification of the ε_C value either the validity of the R_{ct} value

289 could be confirmed or the need for its reevaluation could be identified if, e.g., seasonal changes

290 occur. A distinct influence on the R_{ct} value has been illustrated for changes in temperature, pH,

291 alkalinity and concentration or constitution of NOM.[45] In this context, CSIA offers additional

292 possibilities for the determination of R_{ct} values. However, in its current state, CSIA is still a highly

293 specialized analytical method and remains rather of interest for research purposes and field

294 studies than for a wide application by wastewater treatment plant operators.

295 Moreover, it could also be possible to assess the effectiveness of an O_3 based oxidative process

296 in water or wastewater treatment with CSIA. If there is a minor pollution with benzene or its

297 methylated analogs, CSIA could be used to determine the percentage of degradation initiated by

298 ozone within the entire oxidation process of these potential tracer compounds. Thus, the plant

299 operator would obtain a reliable measure for the evaluation of the overall treatment train.

300 ## Determination of the apparent kinetic isotope effect

301 In the oxidation reaction of O_3 with simple aromatic compounds such as benzene and its

302 analogs, it was postulated that the initial reaction step is the adduct formation of O_3 with the

303 aromatic ring through a monodentate attack of the electrophile O_3 (Scheme S1).[6, 26] This initial

304 reaction step is predicted to be rate determining.[6, 26] Consequently, once the adduct formation

305 has been successful, the subsequent reactions to products are assumed to proceed faster as

306 described elsewhere.[6, 46] For example, possible reactions of an ozone adduct could be the

307 formation of a Criegee ozonide, which further decomposes in water, forming of an oxyl radical

308 and a superoxide anion $\left(O_2^{\bullet -} \right)$ or oxygen transfer resulting in hydroxylation of the aromatic

309 compound and singlet oxygen.[6, 46] However, since these subsequent reactions are predicted to

310   be fast[6, 26], the back reaction from products to adduct is negligible[6, 26] and thus not contributing to

311   the isotopic fractionation of the reaction of the probe compound with O_3.

312   Consequently, the reaction step leading to adduct formation is regarded as the rate determining

313   and, thus, decisive step for isotopic fractionation. This predicted monodentate electrophilic attack

314   of O_3[6, 26] involves one out of at least six carbon atoms present in benzene and its analogs,

315   hence, the nonreactive carbon isotopes will lead to a dilution of the resulting ε_C values. To take

316   this dilution in the average bulk isotopic signature into account the AKIE may be determined

317   according to eq. 1.[12, 24]

318   In eq. 1, only two variables for all benzene analogs may unequivocally be assigned with

319   numerical values (i.e., n and ε_E). For the other two (i.e., x and z) there are several reasonable

320   possibilities (Table 1). In case of benzene all C atoms are chemically identical, making x and z

321   equal n. However, considering toluene (i.e., benzene with only one additional methyl substituent)

322   the assignment of the variables is nontrivial anymore. With regard to the variable x, the methyl

323   substituent may be excluded in general since the electrophile O_3 will attack the slightly activated,

324   electron rich aromatic ring.[6] Thus, there are three remaining possibilities which are exemplified

325   here with toluene:

326   x1. Consideration of all carbon atoms of the aromatic ring (Table 1, Type 1)

327   x2. Consideration of all carbon atoms of the aromatic ring excluding the *ipso*-position (i.e.,

328   position C_1; cf. Figure S9 for carbon numbering) since this one will be subject to steric

329   effects and not favored for adduct formation[26] (Table 1, Type 2)

330   x3. Solely consideration of the *ortho*- and *para*-positions (i.e., positions C_2, C_6 and C_4) which

331   are more favored due to inductive effects (i.e. weak electron donating properties) of the

332   methyl substituent[47] (Table 1, Type 3)

16

333   The variable z specifies the number of equivalent isotopes located in intramolecular competition.

334   The allocation of an unequivocal number may be obvious e.g. in case of transformation

335   reactions limited to the hydrogen isotopes of the methyl group of MTBE[24] but becomes

336   ambiguous for the compounds investigated in this study. Here, different aspects could influence

337   the choice of the variable z (eq. 1). The following options may be considered, again illustrated for

338   toluene as an example:

339   z1. All considered reactive positions are also equal in intramolecular competition. This is true

340   for all cases of a) in Table 1, Type 1-3. In these cases $x = z$, so that these two variables

341   are cancelled out again and n remains the only relevant variable.

342   z2. All positions which are present twice are considered for the variable z, that is the two

343   *ortho*- and the two *meta*-positions (Table 1, Type 1b), Type 2c)) or the two *ortho*-

344   positions (Table 1, Type 3b)).

345   z3. All carbon isotopes of the aromatic ring are involved in the reaction in principle but due to

346   the directing inductive effect of the methyl substituent to *ortho*- and *para*-positions[47] only

347   the two equal *ortho*-positions may be considered for the variable z (Table 1, Type 1d),

348   Type 2e)).

349   The presented options for the variables x and z open different possible ways of approaching the

350   AKIE calculation of the benzene analogs. All options, if applicable, are illustrated for each

351   considered compound in Table 1. Consequently, the question arises which approach of this

352   compilation is chemically meaningful and thus most appropriate. The available literature dealing

353   with isotopic fractionation in abiotic transformation processes of aromatic compounds has not yet

354   dealt with monodentate oxidative reactions in which either $n \neq x$ or $x \neq z$. This means that studies

355   are still missing in which all three variables remain relevant and not two of the implemented

356   variables are cancelled out again.[48-50] In the following, several possible approaches will be

357   presented and discussed, which could be used to identify the most suitable approach for
358   calculation of the AKIE.

359   First of all, it stands out that the option Type 3 is not applicable to all listed compounds in
360   Table 1. Moreover, the obtained results for possibility 3a) or 3b) do not differ numerically from
361   the respective AKIEs of Type 1a) and Type 1b), respectively, and could not be differentiated on
362   this basis. Hence, the option Type 3 is included for the sake of completeness but will not be
363   considered in the following any further.

364   **Scenario 1 - Are all aromatic carbons chemically equivalent? (AKIEs Type 1a) or Type 2a)**
365   **in Table 1):** In general, the substituent(s) of the benzene analogs lead(s) to activation for
366   electrophilic attack of the aromatic ring system through inductive effects.[47] Consequently, the
367   reaction rate constants increase with increasing number of aromatic substituents (Table S1).
368   This increase of reaction rate constants hints to a decrease of the overall required activation
369   energy associated with the potential energy difference between reactant and highest energy
370   transition state.[51] Consequently, a general activation of the aromatic ring system would require
371   consideration of all possibly involved atoms as intramolecular competitors (i.e., $n = z$ and AKIE
372   calculation according to Type 1a) or Type 2a) (Table 1)) so that an AKIE range for the benzene
373   analogs of 1.034 - 1.039 vs. 1.024 for benzene is obtained. This resulting range appears to be
374   very narrow. Furthermore, it would have been expected to observe a trend in the calculated
375   AKIEs of the homologous series, e.g. a decrease from AKIE of benzene to AKIE of mesitylene.
376   However, in the investigated case there seems to be no dependence between the overall
377   reaction rate constants and the determined ε_C values (Figure 1) and the hypothetical AKIEs
378   (Type 1a) or 2a), Table 1), respectively. This behavior is also illustrated by plotting the ε_C values
379   versus the kinetic rate constants of the respective compounds (Figure 2).
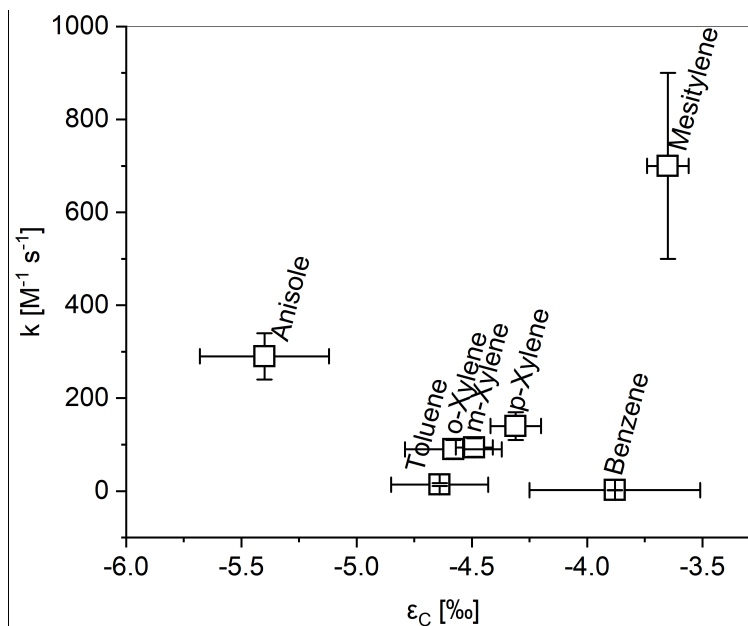
Figure 2: Plot of ε_C values (Table S24) versus the respective rate constants of the ozonation of benzene and its methylated and methoxylated analogs (Table S1)

Scenario 2 - The similarity of *ortho*- and *meta*-positions (AKIEs Type 1b) or Type 2c) in Table 1): The calculation approach of Scenario 1 did not consider the similarity of the two *ortho*- and *meta*-positions, each. Taking toluene as an example, this could be reflected by consideration of all positions affected by intramolecular competition by the *z*-value (eq. 1) without any weighting (i.e., Type 1b) or 2c), Table 1). This approach would regard *ortho*- and *meta*-positions as equal points of attack and disregard the directing inductive effects of the methyl substituents of toluene favoring *ortho*- and *para*-positions over *meta*-positions.[47] Consequently, this approach is not entirely conclusive and will be excluded from further considerations, so that Scenario 3 comes into play.

Scenario 3 - The influence of directive inductive effects (AKIEs Type 1d) or Type 2e) in Table 1): Methyl- and methoxy substituents in aromatic ring systems are expected to cause a directing inductive effect to *ortho*- and *para*-positions[47]. Hence, another possibility is represented by solely including the two *ortho*-positions by the *z*-value for the example of toluene (i.e.

397   Type 1d) or 2e), Table 1). This approach deliberately disregards the non-preferred *meta*-position

398   as possible point of attack. From product studies of other reactions initiated by an electrophilic

399   attack at toluene such as electrophilic bromination or nitration it is known that the meta-products

400   are found with a low percentage of <1 % or 4 %, respectively.[47] Hence, overall product yields of

401   *meta*-products are generally low but, first, will be present within the resulting products so that

402   *meta*-positions cannot be completely excluded and, second, the product yields may not be

403   defined as constant values but may vary depending on the type of electrophile. This discrepancy

404   illustrates that an additional weighting would be required in eq. 1 to represent the individual

405   intramolecular competitive effects inherent e.g. in toluene between the two *ortho*- and *meta*-

406   positions. However, since this weighting is highly compound specific it is not possible to include

407   a universal complementary term in eq. 1.

408   **Scenario 4 - Equal mechanisms necessitate equal AKIEs (AKIE$_{exp, benzene}$ = 1.024 in**

409   **Table 1):** Benzene is the only compound under investigation for which only one possibility of

410   AKIE calculation is given (Table 1). Wijker et al. have found for oxidation of toluene and

411   nitrobenzene by permanganate that similar oxidation pathways show distinctive AKIEs (i.e.,

412   methyl group oxidation versus deoxygenation of the aromatic ring).[49] Following this

413   interpretation, the AKIEs of the benzene analogs should be similar to the AKIE of benzene if the

414   underlying mechanism is similar. Consequently, solely the AKIEs calculated via Type 1b)

415   (Table 1) are in accordance to that approach resulting in a narrow range of AKIE = 1.017 -

416   1.026. However, as described above this approach would regard *ortho*- and *meta*-positions as

417   equal points of attack and disregard the directing inductive effects of the methyl- or methoxy

418   substituents favoring *ortho*- and *para*-positions over *meta*-positions. Consequently, this

419   explanation remains not fully conclusive — similar to the other approaches discussed above.

420   In summary, all four presented scenarios exhibit limitations for the unequivocal determination of

421   the AKIE based on eq. 1. The most implausible option is Scenario 1. Here, all benzene analogs

422　appear in a narrow range (i.e., $\text{AKIE}_{\text{exp, benzene analogs}}$ = 1.034-1.039) which is significantly different

423　from benzene ($\text{AKIE}_{\text{exp, benzene}}$ = 1.024) without observing a consistent trend. Scenario 3 includes

424　the directing inductive effects of the substituents. However, the current form of the AKIE

425　calculation (eq. 1) is not adequate for representing the varying influence for the potential points

426　of an electrophilic attack. Scenario 2, despite excluding the inductive directing effects of the

427　substituents, would be supported by the hypothesis tested in Scenario 4. However, to confirm or

428　disprove each scenario, the primary products would not only need to be identified but also

429　quantified to draw reasonable conclusions. As mentioned above, the quantification of primary

430　reaction products (i.e. muconic or phenolic compounds) is not possible using standard

431　experimental approaches due to their significantly faster reaction rate constants with O_3 with

432　regard to benzene and its analogs. Since an experimental approach for solving this problem

433　appears to be impracticable, the applicability of evidence from theoretical considerations will be

434　evaluated in the following.

Molecular properties from quantum chemistry

436　In the first step the molecule structures were optimized within water as a polarizable medium.

437　Hereafter, the electrostatic potential was mapped onto the electron density and is illustrated in

438　Figure S10. In the various graphic representations, it is possible to draw qualitative conclusions

439　of potential sites more and less favorable for an electrophilic attack, for example of O_3. Because

440　the benzene analogs are not equal in their electrostatic potential, Figure S10 illustrates the

441　necessity of considering a weighting factor for, e.g. *ortho*- and *meta*-positions in toluene or

442　anisole, if AKIE values are calculated.

443　In a second step, a condensed Fukui function (f^{-}_{carbon}, Text S9) was employed to identify

444　potential molecule sites preferred for electrophilic attacks and, additionally, also quantify this

445　preference by means of f^{-}_{carbon} [39, 52-54]. The results are presented in Table S25. In case of

446　benzene and mesitylene no usable results could be obtained with the available means

447　(Text S11). In these two cases LUMO and HOMO are each doubly degenerate. A detailed

448　discussion is given in Text S11. In the remaining cases of toluene, *o*-, *m*-, *p*-xylene and anisole

449　LUMOs and HOMOs are non-degenerate so that determination of f^-_{carbon} was not hampered and

450　was successful.

451　The *ipso*-positions are generally favored. However, steric hindrance might prevent significant

452　attack rates at those positions. In case of toluene and anisole the f^-_{carbon} of the unsubstituted

453　positions are in agreement with the expected preference for the positions para > ortho > meta[47].

454　The unsubstituted positions C_2, C_3, C_5 and C_6 (cf. Figure S9 for carbon numbering) of *p*-xylene

455　are equally attractive for an electrophilic attack. In case of *o*-xylene C_4 and C_5 which combine

456　features of a *meta*- and *para*-position show a much higher reactivity for an electrophilic attack

457　than C_3 and C_6 which are combining features of *meta*- and *ortho*-positions. Finally, *m*-xylene

458　shows high f^-_{carbon} values at the positions C_4 and C_6 which comprise features of *ortho*- and *para*-

459　positions. Position C_5 shows very low reactivity for an electrophilic attack as it could be expected

460　for a perfect *meta*-position. However, the f^-_{carbon} value for position C_2 stands out inconsistently. It

461　would have been expected to find an increased value for reactivity towards an electrophilic

462　attack since this is a true *ortho*-position. Nevertheless, the f^-_{carbon} value for the position C_2 is even

463　lower than for the true *meta*-position C_5.These examples illustrate that a weighting would be

464　required for AKIE calculation and that e.g. *meta*- and *ortho*-positions of toluene or anisole are

465　not equal in intramolecular competition. However, the weighting for the positions which are

466　subject to intramolecular competition appear to be highly specific for the investigated compound

467　set. To that end a generalized weighting factor within eq. 1 for a compound group does not seem

468　reasonable. However, the identified restrictions for the Fukui function of benzene and mesitylene

469　indicate that the Fukui function despite its prior use for similar questions might not be the

470　appropriate tool to fully answer the open questions, that is, to generally quantify the preference

471　of the ozone attack for the different sites.

472   Consequently, in a third step, the optimized molecule structures were used for investigation of

473   the reaction pathways of benzene and its analogs with O_3. The general goal of this approach

474   was to determine geometries of the transition states and the products besides the reactants in

475   order to subsequently calculate the according kinetic isotope effects (KIEs) with the ISOEFF

476   package[37]. Herewith, the obtained theoretical KIEs could be compared to the several AKIE

477   options listed in Table 1 to draw further conclusions and approach a solution of the problem[24].

478   However, numerous attempts for identification of a transition state for the reaction of a reactant

479   (singlet state) plus O_3 (singlet state) in a monodentate attack yielding an adduct (i.e., ozonide)

480   (singlet state) proved to be futile, except for benzene and *p*-xylene. Unfortunately, these two

481   compounds only contribute little to the key question of identifying a weighting factor for

482   intramolecular competition. Nevertheless, KIEs were determined with ISOEFF[37] for these two

483   compounds (Table S26). Both averaged KIEs reflected an *inverse* isotope effect (< 1) as well as

484   the calculated theoretical isotope enrichment factors (ε_C^*) which were positive. Thus, it may be

485   concluded that these quantum chemical models do not yet match with experimental results and

486   require further optimization in the future.

487   We determined transition states for all compounds of interest for the reaction of reactant (singlet

488   state) plus O_3 (triplet state) yielding an adduct (i.e., ozonide) (triplet state) (data not shown). It

489   was not possible to identify any meaningful reason why O_3 should react as electronic triplet state

490   so that this topic was not explored further and the question whether O_3 may react as triplet at all

491   has to be considered in future research. Adamczyk & Paneth have successfully modelled the

492   reaction of benzene plus O_3 (both in electronic singlet state) not as monodentate but as

493   bidentate attack and obtained an ε_C value of −7.36 ‰.[55] This theoretical value differs significantly

494   from the experimental value determined in the present study ($\varepsilon_{C\,(\mathrm{benzene}+O_3)}$ = −3.9 ± 0.4 ‰). This

495   discrepancy between theoretical and experimental values suggests that O_3 does not attack the

496   aromatic ring in a bidentate but in a monodentate attack as it is currently assumed.[6]

497   The question why it was not possible to find meaningful transition states for all benzene analogs

498   in the reaction with O_3 as electronic singlet states remains open. A possible reason might be that

499   O_3 does not attack one specific carbon atom of the aromatic ring, eventually, to form a σ-adduct

500   as it is currently assumed.[6, 26] It might also be possible, that the preliminary π-complex formed in

501   the first place involves all carbons of the aromatic ring system as it has been proposed for $^•OH$[21,

502   56] and other electrophilic aromatic substitutions.[57] In those studies, the π-complex was held

503   accountable for the observed regioselectivity of e.g. the $^•OH$ in reactions with methylated

504   benzene analogs[56] despite its close to diffusion-controlled rate constants (Table S1). In the

505   presented case of this study, such a π-complex would allow directing inductive effects of the

506   substituent(s) to determine the final position of the σ-adduct (i.e., the ozonide) as well. However,

507   in such a case the formation of the π-complex might also be the rate-determining step of the

508   overall reaction. Thus, no specific aromatic carbon bond would primarily be involved in this

509   crucial reaction step so that the observed isotopic fractionation in this study does not originate

510   from chemical bond breakage formation but from π-complex formation.

511   ## Significance

512   This work provides a first systematic evaluation of the utility of CSIA for assessing oxidative

513   processes by two different oxidants (i.e., $^•OH$ and O_3). Our data show that oxidation with O_3 and

514    $^•OH$ of structural moieties in organic contaminants such as benzene and its methylated and

515   methoxylated analogs can lead to significant carbon isotope fractionation. In contrast, the same

516   structural moieties in organic contaminants did not react with ClO_2, and thus, no changes in

517    $^{13}C/^{12}C$ ratios in our probe compounds were observed. These observations suggest that even

518   though several oxidants contribute to contaminant removal in oxidative processes, CSIA may be

519   used selectively to monitor the degradation of target compounds by ozone and to evaluate the

520   suitability of ozonation for specific water treatment applications. The ε_C values derived here
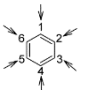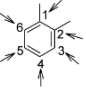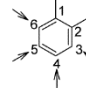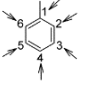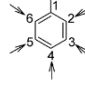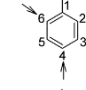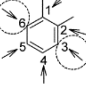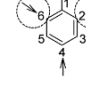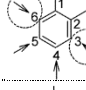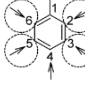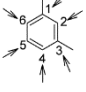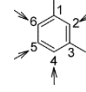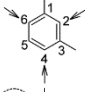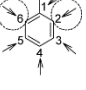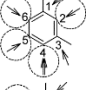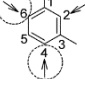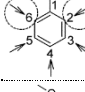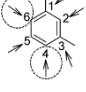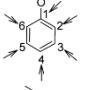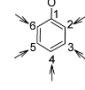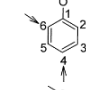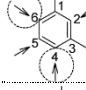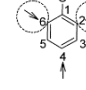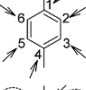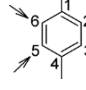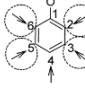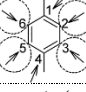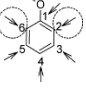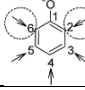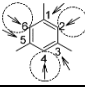
521   provide some guidance for future studies with regard to the magnitude of an anticipated carbon

522   isotope fractionation for comparable oxidation reactions.

523   A general mechanistic interpretation of electrophilic attack by O_3, however, is particularly

524   challenging. Even for simple molecules such as the compounds studied here, interpretation of

525   inductive substituent effects in terms of reactive positions for initial attack by ozone did not

526   reveal a simple pattern of reactivity for *ortho*-, *meta*-, and *para*-substituted benzene analogs that

527   can be used to rationalize the observed isotope fractionation in terms of kinetic isotope effects.

528   Our observations imply that the concept for determination of AKIEs is not applicable in its current

529   form for the considered abiotic reactions (i.e. oxidant reactions with more than one possible point

530   of attack at the (aromatic) target molecule) and needs to be further refined. Further work is

531   warranted such as studies on the oxidation of other benzene analogs for example di- and

532   trimethoxylated benzenes or phenols with O_3 in order to obtain additional mechanistic insights.
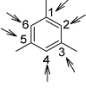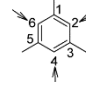
533   Determination of hydrogen additionally to carbon isotope fractionation trends might allow further

534   mechanistic insights. These measures might help to better understand isotope effects of

535   ozonation reactions with organic contaminants in aqueous solution.

Table 1: Possible approaches for calculation of AKIEs (eq. 1) for oxidation of substituted benzenes with O_3. Type 1: x = all aromatic *C*-atoms; Type 2: x = all aromatic *C*-atoms except for *ipso*-position; Type 3: x = only favored *C*-atoms; Numbers in brackets represent the applied variables in the order of (n/x/z) (eq. 1)

	AKIE$_{exp}$	Type 1	Type 2	Type 3		AKIE$_{exp}$	Type 1	Type 2	Type 3
Benzene	1.024 ± 0.002	(6/6/6)	—	—	**o-Xylene**	a) 1.038 ± 0.002	(8/6/6)	(8/4/4)	—
						b) 1.025 ± 0.001	(8/6/4)	—	—
Toluene	a) 1.034 ± 0.002	(7/6/6)	(7/5/5)	(7/3/3)		d) 1.012 ± 0.001	(8/6/2)	—	—
	b) 1.022 ± 0.001	(7/6/4)	—	(7/3/2)		e) 1.019 ± 0.001	—	(8/4/2)	—
	c) 1.027 ± 0.001	—	(7/5/4)	—	**m-Xylene**	a) 1.037 ± 0.001	(8/6/6)	(8/4/4)	(8/3/3)
	d) 1.011 ± 0.001	(7/6/2)	—	—		b) 1.025 ± 0.001	(8/6/4)	—	(8/3/2)
	e) 1.013 ± 0.001	—	(7/5/2)	—		d) 1.012 ± 0.001	(8/6/2)	—	—
Anisole	a) 1.039 ± 0.002	(7/6/6)	(7/5/5)	(7/3/3)		e) 1.018 ± 0.001	—	(8/4/2)	—
	b) 1.026 ± 0.001	(7/6/4)	—	(7/3/2)	**p-Xylene**	a) 1.036 ± 0.001	(8/6/6)	(8/4/4)	—
	c) 1.031 ± 0.002	—	(7/5/4)	—		b) 1.024 ± 0.001	(8/6/4)	—	—
	d) 1.013 ± 0.001	(7/6/2)	—	—	**Mesitylene**	a) 1.034 ± 0.001	(9/6/6)	(9/3/3)	—
	e) 1.015 ± 0.001	—	(7/5/2)	—		b) 1.017 ± 0.001	(9/6/3)	—	—

26

Associated content

Supporting Information

Detailed information on experimental set-ups including calculation approaches plus tabulated kinetic rate constants,a scheme for primary ozone reactions with aromatic compounds, procedures and measurement conditions; background and discussion for Fukui function; figures illustrating carbon isotope fractionation of benzene, toluene, *o*-, *m*-, *p*-xylene, mesitylene and anisole for oxidation with ozone, hydroxyl radicals and chlorine dioxide; discussion of results of chlorine dioxide experiments; tabulated numerical values for the respective isotope enrichment factors; results of quantum chemical calculations including optimized structures, Fukui functions and theoretical position specific ^{13}C-KIE results. This material is available free of charge via the Internet at http://pubs.acs.org.

References

1.	Schwarzenbach, R. P.; Gschwend, P. M.; Imboden, D. M., *Environmental organic chemistry*. 2nd ed.; John Wiley & Sons, Inc.: Hoboken, NJ, USA, 2003.

2.	Skarpeli-Liati, M.; Jiskra, M.; Turgeon, A.; Garr, A. N.; Arnold, W. A.; Cramer, C. J.; Schwarzenbach, R. P.; Hofstetter, T. B., Using nitrogen isotope fractionation to assess the oxidation of substituted anilines by manganese oxide. *Environ Sci Technol* **2011,** *45*, (13), 5596-604.

3.	Solano, F. M.; Marchesi, M.; Thomson, N. R.; Bouchard, D.; Aravena, R., Carbon and hydrogen isotope fractionation of benzene, toluene, and o-xylene during chemical oxidation by persulfate. *Ground Water Monit R* **2018,** *38,* (4), 62-72.

4.	Liu, H.; Bruton, T. A.; Doyle, F. M.; Sedlak, D. L., In situ chemical oxidation of contaminated groundwater by persulfate: Decomposition by Fe(III)- and Mn(IV)-containing oxides and aquifer materials. *Environ Sci Technol* **2014,** *48*, (17), 10330-10336.

5.	Fedrizzi, F.; Ramos, D. T.; Lazzarin, H. S. C.; Fernandes, M.; Larose, C.; Vogel, T. M.; Corseuil, H. X., A Modified Approach for in Situ Chemical Oxidation Coupled to Biodegradation Enhances Light Nonaqueous Phase Liquid Source-Zone Remediation. *Environ Sci Technol* **2017,** *51*, (1), 463-472.

6.	von Sonntag, C.; von Gunten, U., *Chemistry of ozone in water and wastewater treatment*. IWA Publishing: London, UK, 2012.

7.	Gates, D.; Ziglio, G.; Ozekin, K., *State of the science of chlorine dioxide in drinking water*. 1st edition ed.; Water Research Foundation and Fondazione AMGA: Denver, CO, USA, 2009.

8.	Huber, M. M.; Korhonen, S.; Ternes, T. A.; von Gunten, U., Oxidation of pharmaceuticals during water treatment with chlorine dioxide. *Water Res* **2005,** *39*, (15), 3607-17.

9.	Huber, M. M.; Göbel, A.; Joss, A.; Hermann, N.; Löffler, D.; McArdell, C. S.; Ried, A.; Siegrist, H.; Ternes, T. A.; von Gunten, U., Oxidation of pharmaceuticals during ozonation of municipal wastewater effluents: A pilot study. *Environ Sci Technol* **2005,** *39*, (11), 4290-9.

10.	Lee, Y.; von Gunten, U., Quantitative structure–activity relationships (QSARs) for the transformation of organic micropollutants during oxidative water treatment. *Water Res* **2012,** *46*, (19), 6177-6195.

11.	Gottschalk, C.; Libra, J. A.; Saupe, A., *Ozonation of Water and Waste Water - A Practical Guide to Understanding Ozone and its Application*. Wiley-VCH: Weinheim, Germany, 2000.

12.	Elsner, M., Stable isotope fractionation to investigate natural transformation mechanisms of organic contaminants: principles, prospects and limitations. *J Environ Monit* **2010,** *12*, (11), 2005-31.

13.	Schmidt, T. C.; Jochmann, M. A., Origin and fate of organic compounds in water: characterization by compound-specific stable isotope analysis. *Annu Rev Anal Chem (Palo Alto Calif)* **2012,** *5*, 133-55.

14.	Jochmann, M. A.; Schmidt, T. C., *Compound-specific stable isotope analysis*. The Royal Society of Chemistry: Cambridge, UK, 2012.

15.	Aelion, C. M.; Höhener, P.; Hunkeler, D.; Aravena, R., *Environmental isotopes in biodegradation and bioremediation*. CRC Press Taylor & Francis Group: Boca Raton, FL, USA, 2010.

16.	Hofstetter, T. B.; Berg, M., Assessing transformation processes of organic contaminants by compound-specific stable isotope analysis. *TrAC Trend Anal Chem* **2011,** *30*, (4), 618-627.

17.	Meckenstock, R. U.; Morasch, B.; Griebler, C.; Richnow, H. H., Stable isotope fractionation analysis as a tool to monitor biodegradation in contaminated acquifers. *J Contam Hydrol* **2004,** *75*, (3), 215-255.

18.	Elsner, M.; McKelvie, J.; Lacrampe Couloume, G.; Sherwood Lollar, B., Insight into methyl tert-butyl ether (MTBE) stable isotope fractionation from abiotic reference experiments. *Environ Sci Technol* **2007,** *41*, (16), 5693-5700.

600 19.   Maier, M. P.; Prasse, C.; Pati, S. G.; Nitsche, S.; Li, Z.; Radke, M.; Meyer, A.; Hofstetter,
601 T. B.; Ternes, T. A.; Elsner, M., Exploring trends of C and N Isotope fractionation to trace
602 transformation reactions of diclofenac in natural and engineered systems. *Environ Sci Technol*
603 **2016,** *50*, (20), 10933-10942.
604 20.   Willach, S.; Lutze, H. V.; Eckey, K.; Löppenberg, K.; Lüling, M.; Terhalle, J.; Wolbert, J.-
605 B.; Jochmann, M. A.; Karst, U.; Schmidt, T. C., Degradation of sulfamethoxazole using ozone
606 and chlorine dioxide - Compound-specific stable isotope analysis, transformation product
607 analysis and mechanistic aspects. *Water Res* **2017,** *122*, 280-289.
608 21.   Zhang, N.; Geronimo, I.; Paneth, P.; Schindelka, J.; Schaefer, T.; Herrmann, H.; Vogt, C.;
609 Richnow, H. H., Analyzing sites of OH radical attack (ring vs. side chain) in oxidation of
610 substituted benzenes via dual stable isotope analysis (δ(13)C and δ(2)H). *Sci Total Environ*
611 **2016,** *542*, (Pt A), 484-94.
612 22.   Spahr, S.; Bolotin, J.; Schleucher, J.; Ehlers, I.; von Gunten, U.; Hofstetter, T. B.,
613 Compound-specific carbon, nitrogen, and hydrogen isotope analysis of N-nitrosodimethylamine
614 in aqueous solutions. *Anal Chem* **2015,** *87*, (5), 2916-2924.
615 23.   Spahr, S.; von Gunten, U.; Hofstetter, T. B., Carbon, hydrogen, and nitrogen isotope
616 fractionation trends in N-nitrosodimethylamine reflect the formation pathway during
617 chloramination of tertiary amines. *Environ Sci Technol* **2017,** *51*, (22), 13170-13179.
618 24.   Elsner, M.; Zwank, L.; Hunkeler, D.; Schwarzenbach, R. P., A new concept linking
619 observable stable isotope fractionation to transformation pathways of organic pollutants. *Environ*
620 *Sci Technol* **2005,** *39*, (18), 6896-916.
621 25.   Pan, X.-M.; Schuchmann, M. N.; von Sonntag, C., Oxidation of benzene by the OH
622 radical. A product and pulse radiolysis study in oxygenated aqueous solution. *J Chem Soc Perk*
623 *T 2* **1993**, (3), 289-297.
624 26.   Naumov, S.; von Sonntag, C., Quantum chemical studies on the formation of ozone
625 adducts to aromatic compounds in aqueous solution. *Ozone-Sci Eng* **2010,** *32*, (1), 61-65.
626 27.   Hoigné, J.; Bader, H., Rate constants of reactions of ozone with organic and inorganic
627 compounds in water—II: Dissociating organic compounds. *Water Res* **1983,** *17*, (2), 185-194.
628 28.   Fischbacher, A.; Löppenberg, K.; von Sonntag, C.; Schmidt, T. C., A new reaction
629 pathway for bromite to bromate in the ozonation of bromide. *Environ Sci Technol* **2015,** *49*, (19),
630 11714-11720.
631 29.   Sein, M. M.; Golloch, A.; Schmidt, T. C.; Von Sonntag, C., No marked kinetic isotope
632 effect in the peroxone (H2O 2/D2O2 + O3) reaction: Mechanistic consequences.
633 *ChemPhysChem* **2007,** *8*, (14), 2065-2067.
634 30.   Staehelin, J.; Hoigné, J., Decomposition of ozone in water: Rate of initiation by hydroxide
635 ions and hydrogen peroxide. *Environ Sci Technol* **1982,** *16*, (10), 676-681.
636 31.   Foresman, J. B.; Frisch, A., *Exploring chemistry with electronic structure methods*. 3rd
637 edition ed.; Gaussian Inc.: Wallingford, CT, USA, 2015.
638 32.   Frisch, M. J.; Trucks, G. W.; Schlegel, H. B.; Scuseria, G. E.; Robb, M. A.; Cheeseman,
639 J. R.; Scalmani, G.; Barone, V.; Petersson, G. A.; Nakatsuji, H.; Li, X.; Caricato, M.; Marenich, A.
640 V.; Bloino, J.; Janesko, B. G.; Gomperts, R.; Mennucci, B.; Hratchian, H. P.; Ortiz, J. V.;
641 Izmaylov, A. F.; Sonnenberg, J. L.; Williams; Ding, F.; Lipparini, F.; Egidi, F.; Goings, J.; Peng,
642 B.; Petrone, A.; Henderson, T.; Ranasinghe, D.; Zakrzewski, V. G.; Gao, J.; Rega, N.; Zheng,
643 G.; Liang, W.; Hada, M.; Ehara, M.; Toyota, K.; Fukuda, R.; Hasegawa, J.; Ishida, M.; Nakajima,
644 T.; Honda, Y.; Kitao, O.; Nakai, H.; Vreven, T.; Throssell, K.; Montgomery Jr., J. A.; Peralta, J.
645 E.; Ogliaro, F.; Bearpark, M. J.; Heyd, J. J.; Brothers, E. N.; Kudin, K. N.; Staroverov, V. N.;
646 Keith, T. A.; Kobayashi, R.; Normand, J.; Raghavachari, K.; Rendell, A. P.; Burant, J. C.;
647 Iyengar, S. S.; Tomasi, J.; Cossi, M.; Millam, J. M.; Klene, M.; Adamo, C.; Cammi, R.; Ochterski,
648 J. W.; Martin, R. L.; Morokuma, K.; Farkas, O.; Foresman, J. B.; Fox, D. J. *Gaussian 16 Rev.*
649 *C.01*, Wallingford, CT, 2016.
650 33.   Schlegel, H. B., Exploring potential energy surfaces for chemical reactions: An overview
651 of some practical methods. *J Comput Chem* **2003,** *24*, (12), 1514-1527.

652 34. Schlegel, H. B., Moeller-Plesset perturbation theory with spin projection. *J Phys Chem-*
653 *Us* **1988,** *92*, (11), 3075-3078.

654 35. Schlegel, H. B., Potential energy curves using unrestricted Moeller–Plesset perturbation
655 theory with spin annihilation. *J Chem Phys* **1986,** *84*, (8), 4530-4534.

656 36. Scalmani, G.; Frisch, M. J., Continuous surface charge polarizable continuum models of
657 solvation. I. General formalism. *J Chem Phys* **2010,** *132*, (11), 114110.

658 37. Anisimov, V.; Paneth, P., ISOEFF98. A program for studies of isotope effects using
659 Hessian modifications. *J Math Chem* **1999,** *26*, (1), 75-86.

660 38. Steglenko, D. V. *Fukui-function-calculation*, https://github.com/dmsteglenko/Fukui-
661 function-calculation, 2017.

662 39. Contreras, R. R.; Fuentealba, P.; Galván, M.; Pérez, P., A direct evaluation of regional
663 Fukui functions in molecules. *Chem Phys Lett* **1999,** *304*, (5), 405-413.

664 40. Becke, A. D., Density-functional thermochemistry. III. The role of exact exchange. *J*
665 *Chem Phys* **1993,** *98*, (7), 5648-5652.

666 41. Perdew, J. P.; Schmidt, K., Jacob's ladder of density functional approximations for the
667 exchange-correlation energy. *AIP Conf Proc* **2001,** *577*, (1), 1-20.

668 42. Ahad, J. M. E.; Slater, G. F., Carbon isotope effects associated with Fenton-like
669 degradation of toluene: Potential for differentiation of abiotic and biotic degradation. *Sci Total*
670 *Environ* **2008,** *401*, (1), 194-198.

671 43. Elovitz, M. S.; von Gunten, U., Hydroxyl radical/ozone ratios during ozonation processes.
672 I. The Rct concept. *Ozone-Sci Eng* **1999,** *21*, (3), 239-260.

673 44. Kaiser, H.-P.; Köster, O.; Gresch, M.; Périsset, P. M. J.; Jäggi, P.; Salhi, E.; von Gunten,
674 U., Process control for ozonation systems: A novel real-time approach. *Ozone-Sci Eng* **2013,** *35*,
675 (3), 168-185.

676 45. Elovitz, M. S.; von Gunten, U.; Kaiser, H.-P., Hydroxyl radical/ozone ratios during
677 ozonation processes. II. The effect of temperature, pH, alkalinity, and DOM properties. *Ozone-*
678 *Sci Eng* **2000,** *22*, (2), 123-150.

679 46. Mvula, E.; Naumov, S.; von Sonntag, C., Ozonolysis of lignin models in aqueous solution:
680 Anisole, 1,2-dimethoxybenzene, 1,4-dimethoxybenzene, and 1,3,5-trimethoxybenzene. *Environ*
681 *Sci Technol* **2009,** *43*, (16), 6275-6282.

682 47. Vollhardt, K. P.; Schore, N. E., *Organische Chemie; Chapter 16, pp. 787-830*. 5th ed.;
683 Wiley-VCH: Weinheim, Germany, 2011.

684 48. Pati, S. G.; Shin, K.; Skarpeli-Liati, M.; Bolotin, J.; Eustis, S. N.; Spain, J. C.; Hofstetter,
685 T. B., Carbon and nitrogen isotope effects associated with the dioxygenation of aniline and
686 diphenylamine. *Environ Sci Technol* **2012,** *46*, (21), 11844-11853.

687 49. Wijker, R. S.; Adamczyk, P.; Bolotin, J.; Paneth, P.; Hofstetter, T. B., Isotopic analysis of
688 oxidative pollutant degradation pathways exhibiting large H isotope fractionation. *Environ Sci*
689 *Technol* **2013,** *47*, (23), 13459-68.

690 50. Skarpeli-Liati, M.; Pati, S. G.; Bolotin, J.; Eustis, S. N.; Hofstetter, T. B., Carbon,
691 hydrogen, and nitrogen isotope fractionation associated with oxidative transformation of
692 substituted aromatic N-alkyl amines. *Environ Sci Technol* **2012,** *46*, (13), 7189-98.

693 51. Anslyn, E. V.; Dougherty, D. A., *Modern physical organic chemistry*. University Science
694 Books: Sausalito, CA, USA, 2006.

695 52. Parr, R. G.; Yang, W., Density functional approach to the frontier-electron theory of
696 chemical reactivity. *J Am Chem Soc* **1984,** *106*, (14), 4049-4050.

697 53. Bao, Y.; Deng, S.; Jiang, X.; Qu, Y.; He, Y.; Liu, L.; Chai, Q.; Mumtaz, M.; Huang, J.;
698 Cagnetta, G.; Yu, G., Degradation of PFOA substitute: GenX (HFPO–DA ammonium salt):
699 Oxidation with UV/persulfate or reduction with UV/sulfite? *Environ Sci Technol* **2018,** *52*, (20),
700 11728-11734.

701 54. Ayers, P. W.; Levy, M., Perspective on "Density functional approach to the frontier-
702 electron theory of chemical reactivity". *Theor Chem Acc* **2000,** *103*, (3), 353-360.

703   55.   Adamczyk, P.; Paneth, P., Theoretical evaluation of isotopic fractionation factors in
704   oxidation reactions of benzene, phenol and chlorophenols. *J Mol Model* **2011,** *17*, (9), 2285-
705   2296.
706   56.   Kenley, R. A.; Davenport, J. E.; Hendry, D. G., Gas-phase hydroxyl radical reactions.
707   Products and pathways for the reaction of hydroxyl with aromatic hydrocarbons. *J Phys Chem-*
708   *Us* **1981,** *85*, (19), 2740-2746.
709   57.   Olah, G. A., Aromatic substitution. XXVIII. Mechanism of electrophilic aromatic
710   substitutions. *Accounts Chem Res* **1971,** *4*, (7), 240-248.

711